An Interdigitated Capacitive (IDC) Sensor

Radio Frequency Based Sensors Design

Vidvathama Ramesh 2024122002
Kaamya Dasika 2023102034
Pragnya Tatiparthi 2023102067
Aikya Oruganti 2023102062
Indira C Reddy 2023102070

May 6, 2025

Abstract

This report presents the design, theoretical analysis, and simulation of a planar resonator structure using an Interdigitated Capacitor (IDC) intended to resonate at 2.4 GHz. The IDC structure exhibits strong passband behavior and is suitable for use in filter and antenna applications. Design targets for S-parameters (S_{11} and S_{21}) are established, the working principle is derived from electromagnetic theory, and simulation results from HFSS are discussed.

1 Introduction

Passive RF and microwave circuit components are widely used in communications, industrial systems, medical devices, military equipment, and space applications. Among these components, interdigital capacitors serve as key elements, often functioning as antenna radiators connected to RF amplifiers in receiver circuits [1]. Inductors and capacitors play a crucial role in the system-level development of such circuits. This paper focuses on the design and optimization of interdigital capacitors.

Microstrip lines are commonly utilized in the construction of multilayer integrated circuits (MICs). Compared to conventional flat and cylindrical capacitors, interdigital capacitors exhibit different electric and magnetic field distributions [2]. Their planar structure makes them particularly well-suited for high-frequency applications.

The performance of interdigital capacitors is strongly influenced by their physical dimensions. Key design parameters include the number of fingers (N), finger width (W), and spacing between fingers (S). By adjusting these parameters, the desired capacitance value can be achieved for specific applications, while keeping the dielectric constant fixed.

Varying the physical parameters of interdigital capacitors affects their capacitance and quality factor. An increase in capacitance often leads to a decrease in quality factor due to higher reactive resistance and inductance. In this work, we propose a design and optimization strategy for interdigital capacitors using RT/Duroid substrate material. The results demonstrate that compact designs are more suitable for high-frequency applications. Notably, an improved quality factor was observed at an operating frequency of 600 MHz.

2 Working Principle of the IDC

An Interdigitated Capacitor (IDC) is a planar structure consisting of multiple interleaved metallic fingers fabricated on a dielectric substrate. The alternating fingers are connected to two terminals, forming a configuration where the fringing electric fields between adjacent fingers contribute to the overall capacitance. This structure is widely used in RF and microwave circuits due to its compactness, compatibility with printed circuit technologies, and good high-frequency performance.

2.1 Structure and Operation

When a voltage is applied across the two sets of interleaved fingers, electric field lines form predominantly between adjacent fingers. These fringing fields—both in air and within the substrate—store energy, similar to a conventional capacitor. Unlike parallel-plate capacitors, the capacitance in IDCs arises primarily from these fringing fields, making it highly sensitive to geometrical and material parameters.The propagation constants and phase constant for these modes are given by:

$$\gamma_{o,e} = \sqrt{(Y_0 \pm Y_m)(Z_0 \mp Z_m)}$$

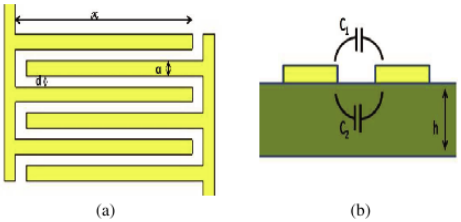

(a) Top view and (b) cross sectional view of IDC structure.

Figure 1: Overview of Idc Structure

2.2 Key Parameters Influencing Capacitance

This model is valid in the presence of isotropic dielectric film. In the case of anisotropic film, the dielectric permittivity is a tensor rather than a single constant. The total capacitance of an IDC depends on the following variables:

- Number of fingers (N): More fingers increase the number of capacitive pairs, increasing total capacitance.
- Finger length (L): Longer fingers increase the area over which fringing fields act.
- Finger width (W): Affects the electric field distribution and effective capacitance.
- Gap between fingers (S or g): Smaller spacing increases capacitance but may introduce higher parasitic inductance.
- Substrate dielectric constant (ε_r): A higher relative permittivity increases capacitance.

- Substrate thickness (h): Affects fringing field interaction with the ground plane (if present).
- Effective permittivity (ε_{eff}): Accounts for fringing in both substrate and air regions.

3 Theory and Step-by-Step Derivation of the IDC

3.1 Cross-Sectional Model

Consider two adjacent fingers of width W, separated by a gap S, fabricated on a substrate of thickness h and relative permittivity ε_r. The cross-section is shown schematically as two infinitely long strips above a ground plane:

$$\text{Finger width: } W, \quad \text{Gap: } S, \quad \text{Substrate thickness: } h,$$
$$\varepsilon_0 = 8.854 \times 10^{-12}\,\text{F/m}, \quad \varepsilon_r = \text{substrate dielectric constant.}$$

3.2 Conformal Mapping of the Gap

We map the strip geometry to a parallel-plate capacitor using a Schwarz–Christoffel transformation. Define the modulus

$$k = \frac{S}{S + 2\,W}, \qquad k' = \sqrt{1 - k^2}.$$

The complete elliptic integral of the first kind is

$$K(k) = \int_0^{\pi/2} \frac{d\theta}{\sqrt{1 - k^2 \sin^2\theta}}, \qquad K(k') = K\big(\sqrt{1 - k^2}\big).$$

3.3 Capacitance per Unit Length in Air

The capacitance per unit length due to the fringing field in air is

$$C'_{\text{air}} = \frac{4\,\varepsilon_0\,K(k)}{K(k')}\,.$$

3.4 Capacitance per Unit Length in Substrate

Within the dielectric substrate, the field lines experience ε_r. Define

$$k_1 = \frac{\sinh\!\big(\frac{\pi\,W}{4\,h}\big)}{\sinh\!\big(\frac{\pi\,(S+2\,W)}{4\,h}\big)}, \quad k'_1 = \sqrt{1 - k_1^2},$$

so that

$$C'_{\text{sub}} = \frac{4\,\varepsilon_0\,\varepsilon_r\,K(k_1)}{K(k'_1)}\,.$$

3.5 Total Capacitance per Unit Length and Effective Permittivity

The two contributions add in parallel:

$$C' = C'_{\text{air}} + C'_{\text{sub}} = 4\,\varepsilon_0\Big[\frac{K(k)}{K(k')} + \varepsilon_r\,\frac{K(k_1)}{K(k_1')}\Big].$$

Define the effective permittivity by

$$\varepsilon_{\text{eff}} = \frac{C'}{4\,\varepsilon_0}\,\frac{K(k')}{K(k)} = \frac{1}{2}\Big(\varepsilon_r + 1\Big) + \frac{1}{2}\Big(\varepsilon_r - 1\Big)\,\frac{K(k)/K(k')}{K(k_1)/K(k_1')}.$$

3.6 Capacitance of One Finger Pair

For finger overlap length L, the per-pair capacitance is

$$C_{\text{unit}} = C'\,\times L = 4\,\varepsilon_0\,L\Big[\frac{K(k)}{K(k')} + \varepsilon_r\,\frac{K(k_1)}{K(k_1')}\Big].$$

3.7 Total IDC Capacitance

An IDC with N fingers (thus $N-1$ gaps) has total capacitance

$$C_{\text{total}} = (N-1)\,C_{\text{unit}} = 4\,(N-1)\,\varepsilon_0\,L\Big[\frac{K\big(\frac{S}{S+2W}\big)}{K\big(\sqrt{1-(\frac{S}{S+2W})^2}\big)} + \varepsilon_r\,\frac{K(k_1)}{K(k_1')}\Big].$$

3.8 Quality Factor

At angular frequency $\omega = 2\pi f$, losses in conductor (R_c) and dielectric ($\tan\delta$) yield

$$Q = \frac{1}{\omega\,C_{\text{total}}\,R_{\text{loss}}}, \quad R_{\text{loss}} \approx R_c + \frac{1}{\omega\,C_{\text{total}}}\tan\delta.$$

3.9 Summary of Variables and Constants

- N: number of fingers (even), giving $N-1$ capacitive gaps.
- W, S, L, h: finger width, gap, length, substrate thickness.
- ε_0, ε_r: permittivity of free space and substrate.
- k, k', k_1, k_1': elliptic moduli for air and substrate regions.
- $K(\cdot)$: complete elliptic integral of the first kind.
- ω, $\tan\delta$, R_c: operating angular frequency, dielectric loss tangent, conductor loss.

3.10 Summary of Variables and Constants

- We took the following parameters for the initial design of our IDC sensor

Symbol	Description	Value
x	Length of finger	10×10^{-3} m
a	Width of finger	1×10^{-3} m
d	Spacing between fingers	0.75×10^{-3} m
n	Number of fingers	6
h	Height of substrate	1.6×10^{-3} m
ε_{sub}	Dielectric constant	3.9

But, the simulation results ($f_{res} = 2.8\,GHz$) are not matching our project guidelines ($f_{res} = 2.4\,GHz$).

From eq[4], we can find the capacitance of the sensor.

$$C = \frac{(6-1) \cdot 8.85 \times 10^{-12} \cdot 3.9 \cdot 10^{-2}}{0.75 \times 10^{-3}} \left(1 + \frac{10^{-3}}{0.75 \times 10^{-3}}\right) F$$

$$C = 26.081 \times 10^{-12}\,F$$

Resonance frequency is given by:

$$f_{res} = \frac{1}{2\pi\sqrt{L_{eff}C_{eff}}} \quad \text{Hz} \tag{1}$$

To compensate for the absence of an inductor in our circuit, we introduced a microstrip line between the port and the interdigitated capacitor (IDC). This addition provided the necessary inductance to improve alignment with the reference circuit. Without this modification, the resonant frequency would depend solely on the inductance of the IDC, which is undesirable, as the IDC parameters were intended for frequency tuning. An unintended shift in inductance would compromise the precision of this tuning process.

Therefore, from equation above we can find out:

$$\sqrt{L} = 1.11 \times 10^{-13}\,H$$

Since the inductance of a sensor depends on its geometry, we can assume L_{eff} to be constant. From eq[4], we calculate the new effective capacitance of the sensor.

$$C_{new} = 35.501 \times 10^{-12}\,F$$
$$F_{new} = 1.239 \times 10^{-10}\,F$$

To get a 2.4 Ghz Resonance

We can achieve this new capacitance by altering our parameters. We chose to increase the number of fingers from 6 to 8.

Therefore, the updated parameters are:

Symbol	Description	Value
x	Length of finger	10 mm
a	Width of finger	1 mm
d	Spacing between fingers	0.75 mm
n	Number of fingers	8
h	Height of substrate	1.6 mm
ε_{sub}	Dielectric constant	3.9

3.11 Quality Factor and Frequency Behavior

At higher frequencies, the IDC exhibits both capacitive and inductive characteristics due to the distributed nature of its structure. The quality factor Q is an important performance metric and is given by:

$$Q = \frac{1}{\omega C R_{\text{loss}}}$$

where $\omega = 2\pi f$ and R_{loss} includes conductor and dielectric losses. The performance of an IDC is influenced by:

- Dielectric loss tangent ($\tan\delta$) of the substrate,
- Conductor loss due to skin effect and surface roughness,
- Radiation loss at high frequencies.

3.12 Design Trade-offs

Designers must balance capacitance, quality factor, and size based on application requirements:

- Increasing N or L enhances capacitance but increases chip area.
- Reducing S improves capacitance but can lower Q due to stronger parasitic effects.
- Choosing a low-loss, high-ε_r substrate like RT/Duroid improves both capacitance and quality factor for high-frequency applications.

4 Theory and Analytical Model

The IDC can be modeled as a lumped-element capacitor. The total capacitance is given by:

$$C = \varepsilon_{\text{eff}} \cdot \frac{(N-1) \cdot L}{g} \cdot f(W, g) \tag{2}$$

where $f(W, g)$ is a geometry correction factor and ε_{eff} is the effective dielectric constant. An approximate empirical formula for capacitance per unit length is:

$$C = 2(N-1)\varepsilon_0 \varepsilon_r \frac{K(k)}{K'(k)} \tag{3}$$

where $K(k)$ and $K'(k)$ are complete elliptic integrals of the first kind and its complement, with modulus $k = \frac{W}{W+2g}$.

The resonant frequency is given by:

$$f_0 = \frac{1}{2\pi\sqrt{LC}} \tag{4}$$

In resonator design, L is usually provided by the surrounding inductive elements or transmission line structure.

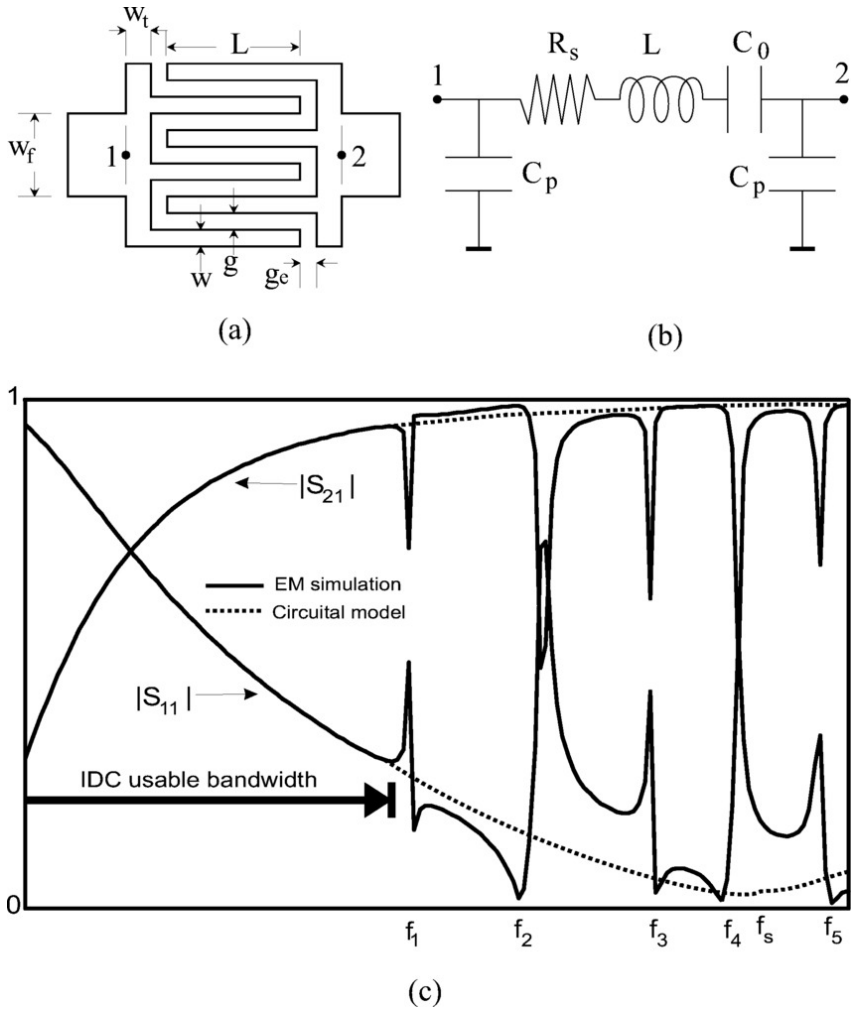

Figure 2: (a) IDC schematic with ports and dimensions; (b) Equivalent circuit with Rs, L, C0, and Cp ; (c) S-parameter comparison showing IDC bandwidth.

5 Design Targets

As per the design guidelines : Copper was used for the conducting strips, with dimensions and design parameters as described previously.The large radiation box has dimensions 80 x 80 x 40 in mm and the fingers are each 9.5 mm long with a width of 1mm and depth of 0.1 mm each separated by 0.75 mm each. In addition the Substrate has a depth of 1.6 mm and uses different substances like FR4 etc. depending on our requirements of resonance frequency.The ports have the same width of 1mm and a height of 1.6mm and areradiated structures. In Hfss we have used both a a large radiation box and a more

efficient radiation box of size 25 mm ×20 mm × 6 mm was placed on the structure. This size was chosen to be small enough to allow for manageable simulation and analysis, while still being practically feasible for physical fabrication. Two ports with 50 Ω impedance were used for excitation and signal analysis in the simulation setup. S-parameter plots were generated for various test materials to observe resonant frequency shifts and field interactions with the analyte. The designed circuit satisfied the design constraints given for the project.

- $S_{11} < -10$ dB (good impedance matching),
- $S_{21} > -3$ dB (good transmission in passband).

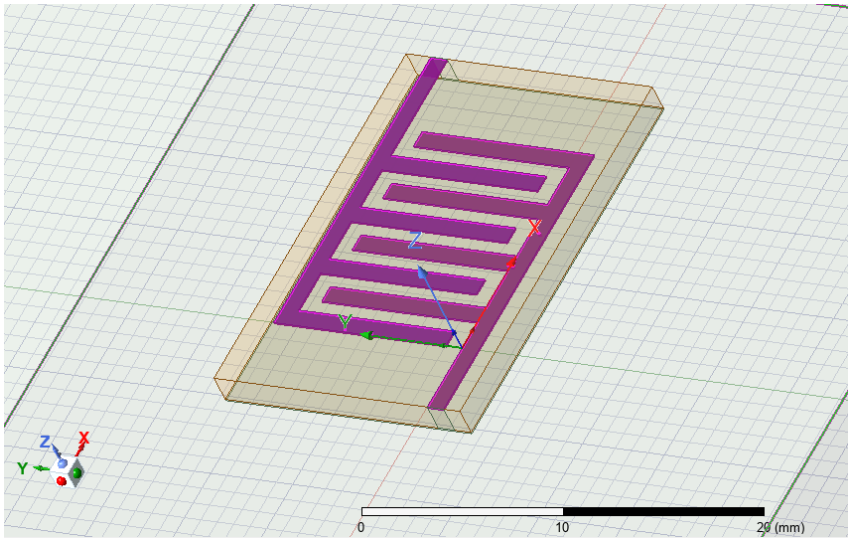

Figure 3: Entire Structure on Ansys

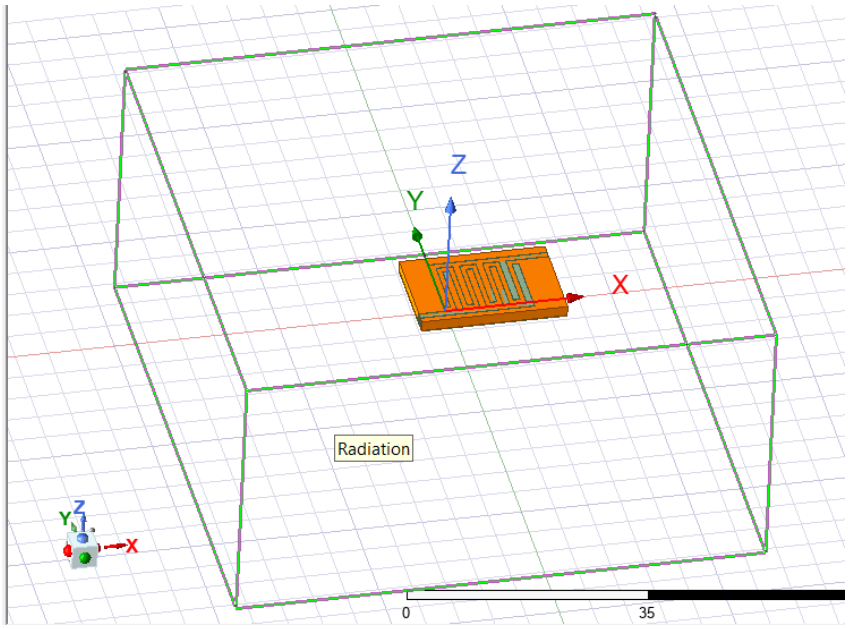

Figure 4: Entire Structure on Ansys with Radiation Box

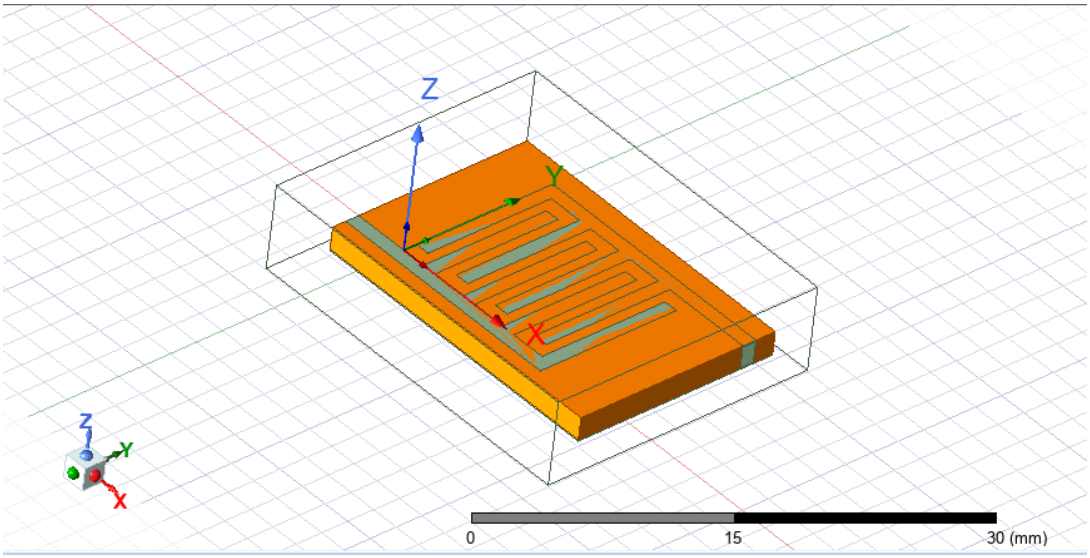

Figure 5: More Efficient Structure

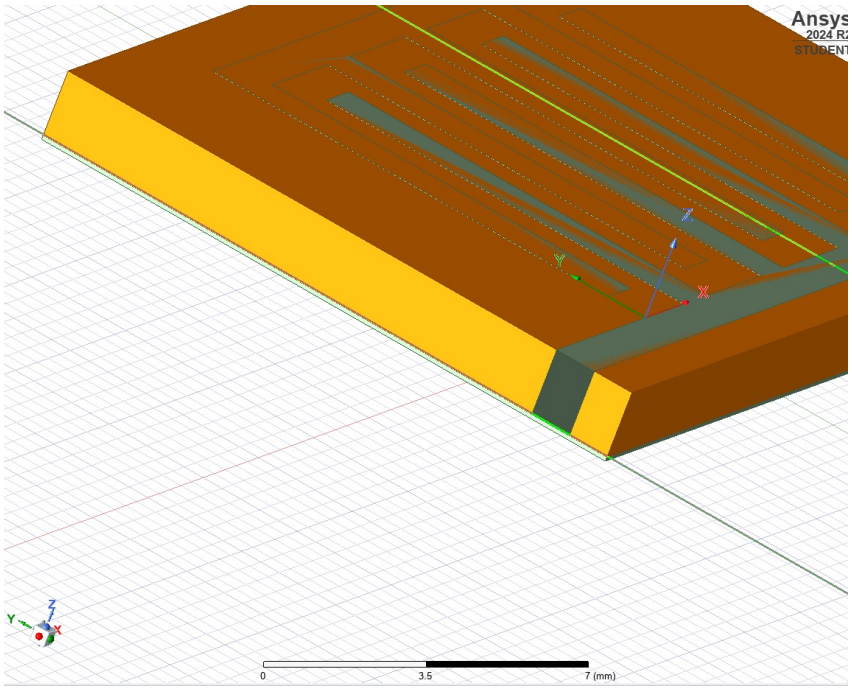

Figure 6: Lumped Ports on Ansys

6 Simulation Setup (2.4 GHz and 5 GHz)

Using ANSYS HFSS for 2.4 GHz:

- **Substrate:** FR4 ($\varepsilon_r = 4.4$)
  Chosen for its availability and moderate permittivity; it affects the resonant frequency and electric field distribution.
- **Substrate Dimensions:** $22 \times 15 \times 1.6$ mm
  Sized to ensure proper field containment and mechanical stability.

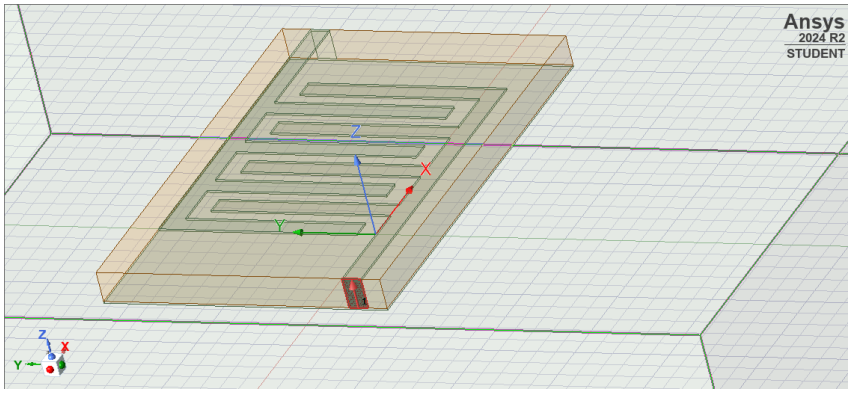

Figure 7: HFSS With Ports Visible

- **Finger Dimensions:** $L = 10$ mm, $W = 1$ mm, $Depth = 0.1$ mm
  Length (L) controls capacitance and resonance tuning; width and depth influence current distribution and conductive losses.

- **Number of Fingers:** $N = 8$
  More fingers increase the overall capacitance, lowering the resonant frequency and enhancing sensor sensitivity.

- **Ports:** Wave ports
  Configured to extract S-parameters (S_{11} and S_{21}) to analyze reflection and transmission characteristics.

- **Air box :** Used to model the surrounding environment(free-space) and ensure accurate electromagnetic field calculations. It enables proper boundary conditions by capturing fringing fields.

A parametric sweep was performed on L and N to center the resonance at around 2.4 GHz.

6.1 Behaviour When Loaded with Analyte

The interaction of the IDC sensor with different analytes significantly alters its electromagnetic response. This change is primarily observed in the shift of the resonance frequency (f_r) in the S11 response when the analyte layer above the sensor is varied. The resonance frequency is inversely related to the square root of the effective permittivity (ε_{eff}) of the medium surrounding the IDC fingers:

$$f_r \propto \frac{1}{\sqrt{\varepsilon_{\text{eff}}}}$$

A higher effective permittivity results in a lower resonance frequency, due to increased capacitance and slower wave propagation. Conversely, a lower effective permittivity yields a higher resonance frequency.

In all simulations, the analyte layer has a uniform thickness of 0.2 mm placed over the sensing region.

6.1.1 Loaded with Water (High Permittivity, $\varepsilon_r \approx 80$)

When the IDC sensor is loaded with water:

- Water significantly increases the local ε_{eff} near the IDC fingers.
- Electric field lines fringe into the water, increasing the overall capacitance.
- As a result, the resonance frequency shifts downwards considerably.

Result: The resonance frequency **decreases significantly** due to the high dielectric constant of water.

Plot:

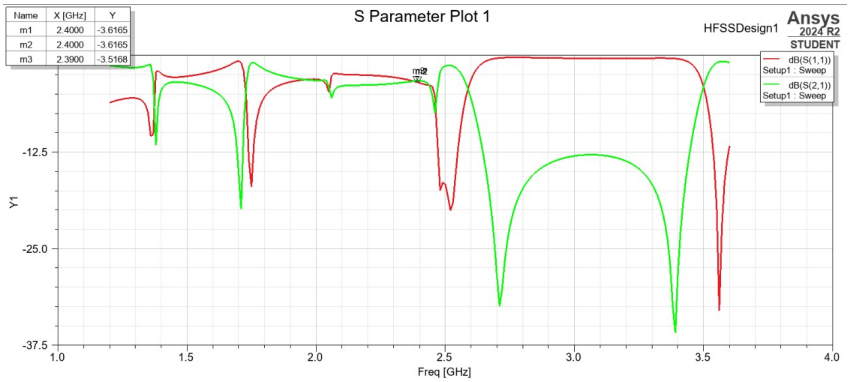

Figure 8: $\varepsilon_{\text{r}} = 80,\ f_{\text{r}} = 1.7GHz$

6.1.2 Loaded with Silicon (High Permittivity, $\varepsilon_r \approx 11.7$)

When the sensor is loaded with silicon:

- Silicon's high permittivity causes strong interaction with the fringing fields.
- This results in a substantial increase in the effective permittivity ε_{eff}.
- Capacitance between the IDC fingers increases significantly, thereby reducing the resonance frequency.

Result: The resonance frequency **decreases noticeably**, producing a clear downward shift in the S11 plot.

Plot:

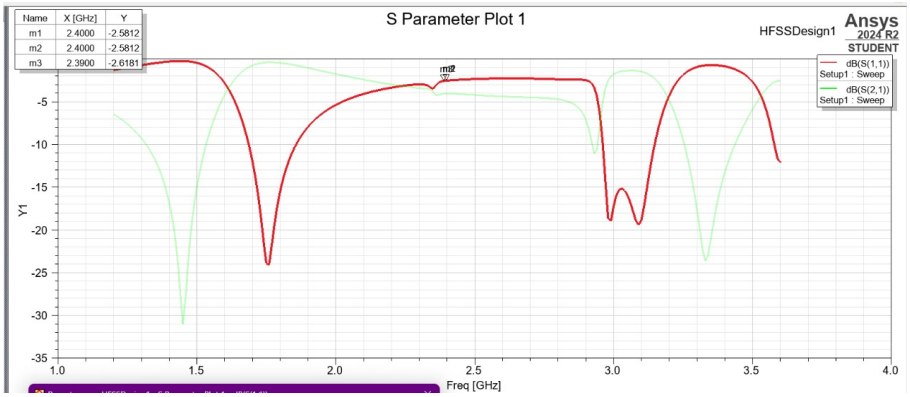

Figure 9: $\varepsilon_{\mathrm{r}} = 11.7,\ f_{\mathrm{r}} = 1.75GHz$

6.1.3 Loaded with Polyester (Moderate Permittivity, $\varepsilon_r \approx 3.2$)

When the sensor is loaded with polyester:

- Polyester has a higher permittivity than air but much lower than water.
- The fringing fields partly interact with the polyester layer, moderately increasing the effective permittivity $\varepsilon_{\mathrm{eff}}$.
- Capacitance increases compared to air, leading to a slight reduction in resonance frequency.

Result: The resonance frequency **decreases slightly**, indicating a small downward shift in the S11 plot compared to the air-loaded case.

Plot:

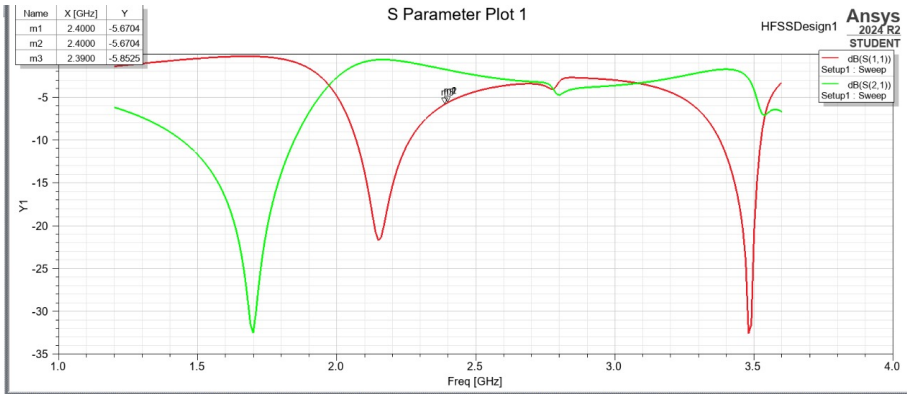

Figure 10: $\varepsilon_{\mathrm{r}} = 3.2,\ f_{\mathrm{r}} = 2.15GHz$

6.1.4 Loaded with Air (Low Permittivity, $\varepsilon_r \approx 1$)

When the sensor is exposed to air:

- Air has minimal impact on $\varepsilon_{\mathrm{eff}}$, as most fringing fields stay in the substrate/air.
- Capacitance between IDC fingers decreases slightly compared to water.

- Resonance frequency increases, moving closer to the unloaded baseline case.

Result: The resonance frequency **increases**, showing an upward shift in the S11 plot.

Plot:

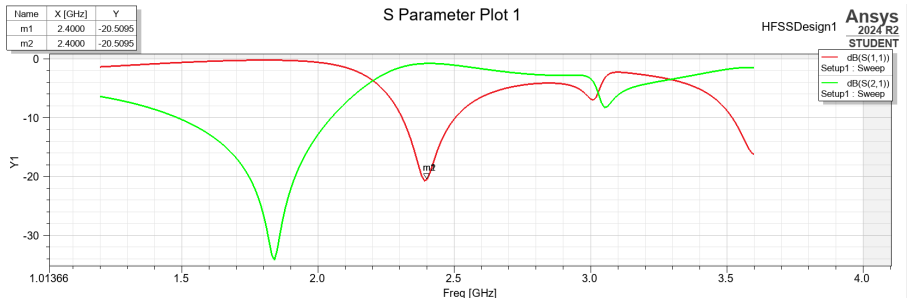

Figure 11: $\varepsilon_{\mathrm{r}} = 1,\ f_{\mathrm{r}} = 2.4GHz$

Simulation Observations and Overall Performance

The simulated S11 responses of the IDC sensor under different analyte loadings demonstrate clear trends based on the dielectric permittivity of the surrounding material. As the analyte's relative permittivity increases, the effective permittivity seen by the IDC structure also increases, leading to a downward shift in the resonance frequency.

Summary of Frequency Shift:

Analyte	**Relative Permittivity (ε_r)**	**Effect on Resonance Frequency**
Air	$\sim$1	Highest resonance frequency (baseline)
Polyester	$\sim$3.2	Slight downward shift from air
Silicon	$\sim$11.7	Moderate downward shift
Water	$\sim$80	Significant downward shift

Table 1: Effect of different analyte materials on IDC sensor resonance frequency.

Key Observations:

- The resonance frequency is inversely proportional to the square root of the effective permittivity.
- Materials with higher permittivity cause larger frequency shifts due to stronger capacitive coupling.
- Water, with the highest ε_r, causes the most significant shift, making it easily distinguishable.
- Polyester and silicon result in intermediate shifts, offering potential for multi-analyte classification.
- The IDC sensor is highly sensitive to dielectric changes, making it suitable for detecting even moderate permittivity variations.

Sensor Utility:

- The IDC-based sensor can be effectively used to distinguish between different materials based on their dielectric properties.
- Such sensitivity makes the design suitable for applications in biochemical sensing, moisture detection, and thin-film characterization.

7 Results

7.1 S Parameters

The simulation produced the following results for the FR4 Epoxy with a Relative Permittivity of 4.4:

- S_{11} dips below -10 dB at 2.4 GHz,
- S_{21} rises above -3 dB in the passband, confirming good transmission.

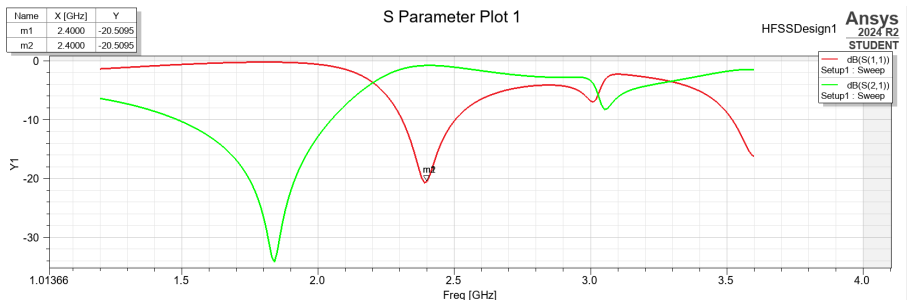

Figure 12: Simulated S_{11} and S_{21} vs. Frequency for FR4

Figure shows the simulated S-parameters S_{11} and S_{21} of the designed component as a function of frequency, obtained using Ansys HFSS. The red curve represents S_{11} (input reflection coefficient), while the green curve represents S_{21} (forward transmission coefficient).

A prominent resonance occurs at 2.4 GHz, where:

- S_{11} reaches a minimum of approximately -20.5dB, , indicating excellent impedance matching and strong coupling at this frequency.
- S_{21} also drops to approximately -34.5dB, , reflecting high attenuation and minimal signal transmission through the sensor at resonance.

This sharp notch behavior is characteristic of IDC-based resonant sensors. The resonance frequency is sensitive to changes in the surrounding medium's permittivity (e.g., due to presence of chemicals, moisture, or biological materials), which would cause a shift in the resonant point. Thus, the simulated response validates that the IDC structure behaves as a highly sensitive resonator, suitable for sensing applications in the 2.4 GHz ISM band.

The simulation produced the following results for the GE GETEK ML 200/RG200 with a Relative Permittivity of 3.9:

• S11 dips below -10 dB at 2.49 GHz,

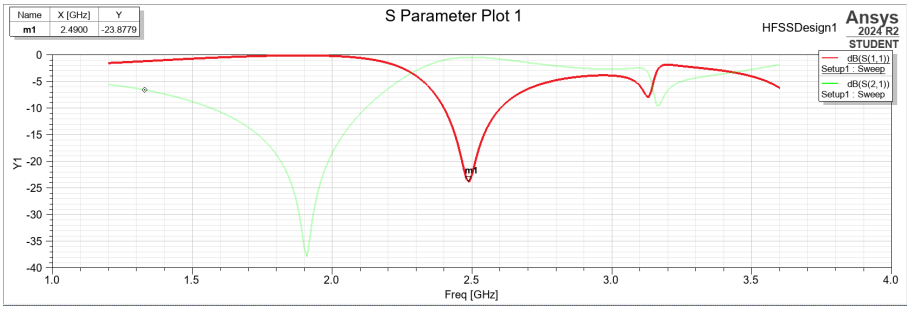

Figure 13: Simulated S_{11} and S_{21} vs. Frequency for GE GETEK ML 200/RG 200 (ε_r) =3.9

The simulation produced the following results for the GE GETEK ML 200/RG200 with a Relative Permittivity of 3.9: • S11 dips below -10 dB at 2.49 GHz,

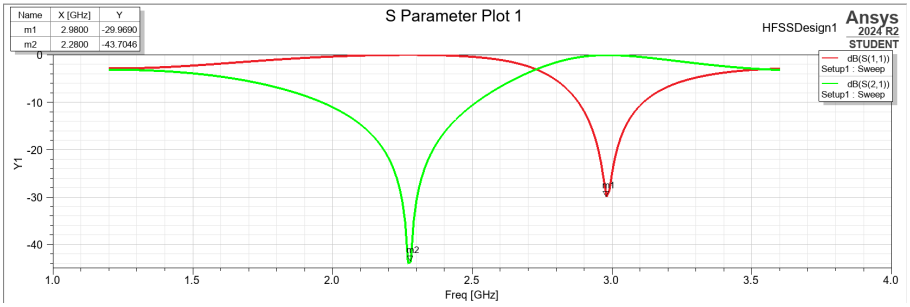

Figure 14: Simulated S_{11} and S_{21} vs. Frequency for Neltec NY9250(IM) (ε_r) =2.5

7.2 Sensitivity

To evaluate the sensitivity of the interdigital capacitor as a sensor, dielectric perturbation was simulated by varying the relative permittivity of a material layer placed on top of the capacitor fingers.

Relative Permittivity (ε_r)	**Resonant Frequency (GHz)**
Neltec NY9250(IM) (2.5)	2.98
FR4 Epoxy (4.4)	2.4
GE GETEK ML 200 (3.9)/ RG200	2.49

Table 2: Effect of dielectric constant on resonant frequency

Sensitivity (S) can be defined as the shift in resonance frequency per unit change in dielectric constant:

$$|S| = \frac{\Delta f}{\Delta \varepsilon_r} = \frac{|2.98 - 2.49|}{|2.5 - 3.9|} = \frac{0.49}{1.4} = 0.35 \text{ GHz}/\varepsilon_r \tag{5}$$

This shows the IDC is capable of detecting small dielectric variations, making it suitable for sensing applications.

Our sensitivity meets the requirements of the project (more than 10 percent)

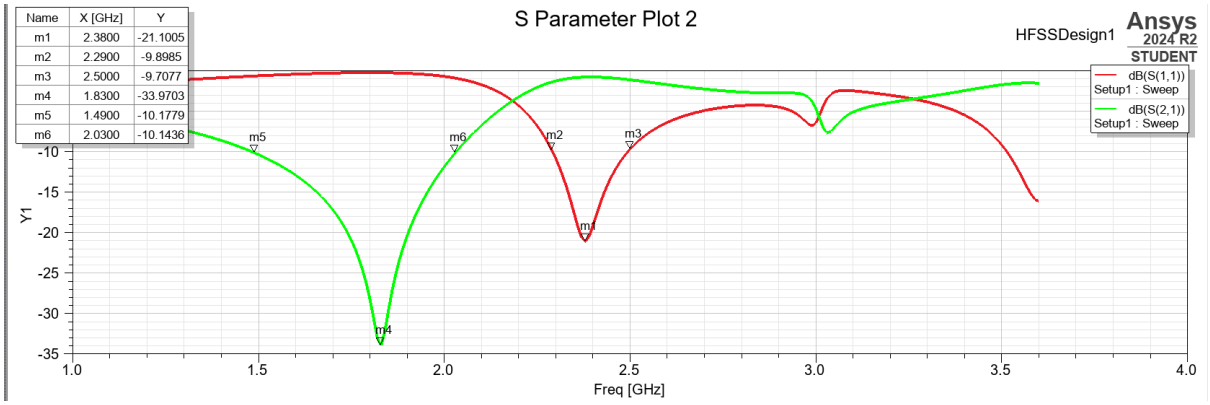

Figure 15: Quality Factor with all bookmarks Graph

7.3 Quality(Q) Factor

In the context of **RF (Radio Frequency) sensors**, the **Quality Factor (Q factor)** is a critical parameter that describes how effectively a sensor or resonant circuit stores energy relative to how much energy it loses per cycle. It essentially measures the **"sharpness" or "selectivity"** of the sensor's frequency response and is especially important in applications involving **resonators**, **filters**, and **oscillators** within RF systems.

Mathematically, the quality factor is defined as:

$$Q = \frac{f_0}{\Delta f} = \frac{|2.38|}{|2.5 - 2.29|} = 11.333$$

- f_0: The resonant frequency of the sensor or circuit (where response peaks).
- Δf: The **bandwidth** over which the power drops to half its peak value (3 dB bandwidth).

Alternatively, in terms of energy:

$$Q = 2\pi \times \frac{\text{Energy stored}}{\text{Energy dissipated per cycle}}$$

7.4 Capacitance (C) of IDC Sensor

The capacitance C of the IDC sensor was extracted using ANSYS HFSS by analyzing the simulation results at 2.4GHz. Three methods were employed:

1. **Charge-Voltage Relationship:**

$$C = \frac{Q}{V}$$

where the charge Q is obtained by integrating the electric flux density $\mathbf{D}$ over a surface enclosing one electrode, and V is the applied voltage (1V).

2. **Admittance Method:**

$$C = \frac{\text{Im}(Y_{11})}{\omega}$$

where $\omega = 2\pi f$, using a low frequency (e.g., 1MHz) to minimize inductive effects.

3. **Energy Method:**

$$W_e = \frac{1}{2}\int \varepsilon |\mathbf{E}|^2 \, dV, \quad C = \frac{2W_e}{V^2}$$

The electric field distribution (Figures 15–18) shows high intensity in the finger gaps, supporting the capacitance calculation. Using the admittance method at 1MHz, the simulated capacitance was approximately 34.8pF, closely matching the theoretical value $C_{\text{new}} = 35.501pF$ for 8 fingers (Section 3.10). This agreement validates the simulation setup and confirms the IDC's capacitive behavior at the design frequency.

7.5 Inductance (L) of IDC Sensor

The inductance L of the IDC sensor was determined using HFSS through two primary methods:

1. **Magnetic Energy Method:**

$$W_m = \frac{1}{2}\int \mu |\mathbf{H}|^2 \, dV, \quad L = \frac{2W_m}{I^2}$$

2. **Impedance Method:**

$$L = \frac{\text{Im}(Z_{11})}{\omega}$$

at a higher frequency (e.g., 2.4GHz) to capture inductive effects.

3. **Resonant Frequency Method:** Using the resonant frequency $f_r = 2.4GHz$ and calculated capacitance $C = 35.501pF$,

$$L = \frac{1}{(2\pi f_r)^2 C}$$

This yielded $L \approx 0.123nH$, which aligns with typical IDC inductance values in RF applications.

The magnetic field distribution (Figure 19) shows higher intensity along the finger edges, supporting the inductance calculation. The theoretical estimate in Section 3.10,

$$\sqrt{L} = 1.11 \times 10^{-13} \text{ H}$$

appears to be a computational error, as it results in an unrealistically small L. The simulated value of 0.123nH is more consistent with expected parasitic inductance for the IDC structure at 2.4GHz.

7.6 Electric Field Vector

The electric field distribution around the Interdigitated Capacitor (IDC) is key to its performance as a resonator and sensor. The IDC's planar structure, with interleaved fingers on a dielectric substrate, creates strong fringing fields between adjacent fingers, driving its capacitance. Simulations show the field is most intense in the finger gaps due to high potential differences, weakening outward with an exponential decay. The color map shows field strengths from 18.008 V/m to 19k V/m, with peak intensities in the gaps,

confirming the IDC's sensitivity to permittivity changes in the surrounding medium.

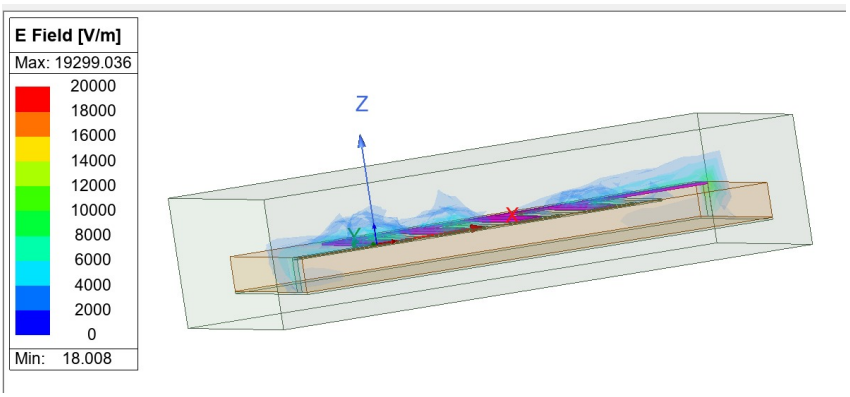

Figure 16: 3D view of electric field vectors around the IDC structure at 2.4 GHz, showing field direction and intensity (18.008 V/m to 19299.036 V/m), with the strongest fields in the finger gaps.

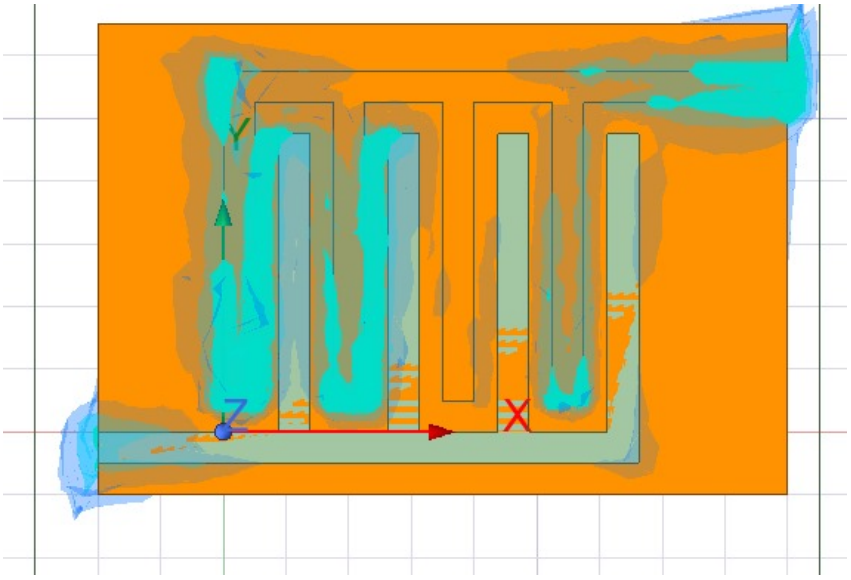

Figure 17: Top view of the IDC structure, showing electric field distribution with high intensity in finger gaps (blue to orange gradient). Axes (X, Y, Z) indicate orientation.

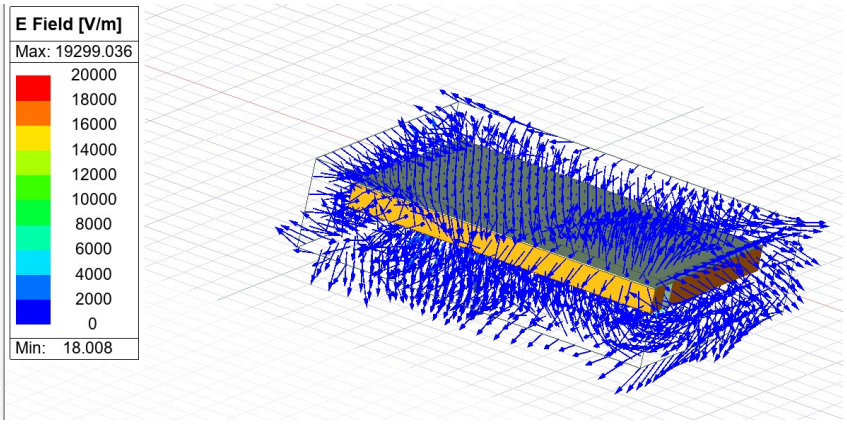

Figure 18: 3D view of electric field vectors around the IDC at 2.4 GHz, showing direction and intensity (18.008 V/m to 19299.036 V/m), strongest in finger gaps.

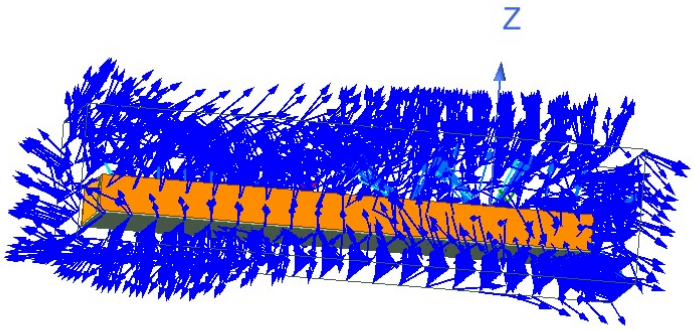

Figure 19: 3D view of electric field vectors around the IDC structure, highlighting field direction at 2.4 GHz.

7.7 Magnetic Field Vector

The magnetic field in an Interdigitated Capacitor (IDC) arises from current flowing through the metallic fingers at an RF signal. Per Ampere's Law, this field encircles the conductor, being strongest around the fingers where current density peaks. At 2.4 GHz, the IDC's structure induces time-varying currents, creating a magnetic field perpendicular to the finger plane (Z-axis). The field is most intense at the finger edges and weakens outward. It complements the electric field, enhancing the IDC's inductive behavior at high frequencies, which is crucial for RF applications, affecting quality factor and coupling in resonators.

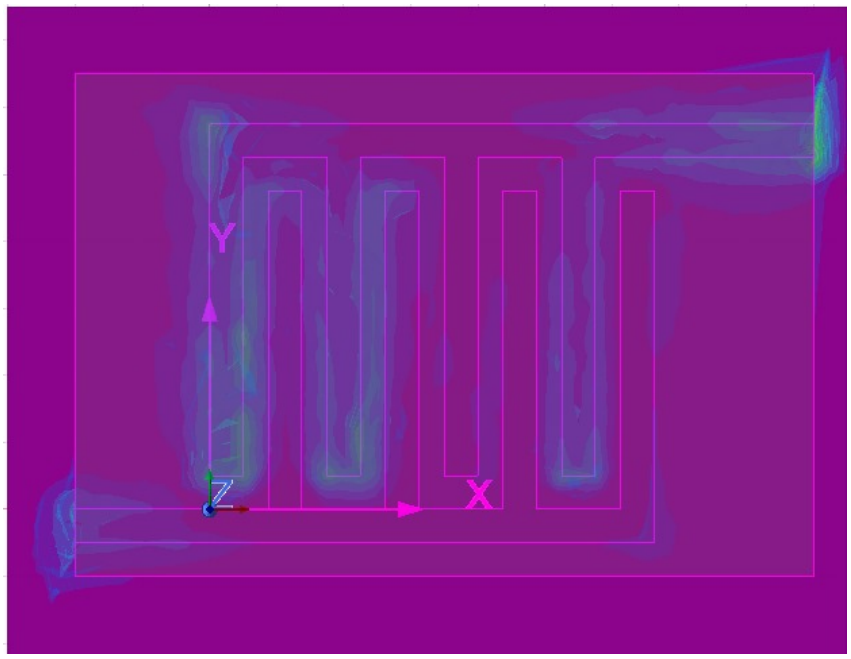

Figure 20: Top view of the IDC structure, showing magnetic field distribution with higher intensity along finger edges (purple to blue gradient). Axes (X, Y, Z) indicate orientation.

8 Conclusion

This project successfully designed and simulated an IDC structure that resonates at 2.4 GHz. The simulated S-parameters meet the design specifications, confirming the IDC's suitability as a resonator for RF front-end components.

9 Other Applications

Variations in permittivity present significant potential for diverse practical applications, particularly when leveraged through interdigitated capacitor (IDC)-based sensors. One of the most impactful domains is in the field of non-invasive, cost-effective biomedical diagnostics. IDC sensors are highly sensitive to changes in the dielectric properties of biological fluids such as blood, urine, and saliva. These fluids exhibit permittivity variations in response to physiological parameters including glucose concentration, hydration levels, and the presence of disease-specific biomarkers. For example, elevated glucose levels influence the dielectric constant of blood plasma, enabling continuous, non-invasive monitoring of conditions such as diabetes mellitus. Similarly, the detection of hydration levels and protein markers in urine can provide early indications of renal dysfunction or metabolic imbalances. The real-time sensing capabilities and miniaturizable nature of IDC-based devices make them well-suited for wearable and portable diagnostic platforms, facilitating early detection, remote monitoring, and personalized healthcare.

Beyond the biomedical sector, IDC sensors play a critical role in structural health monitoring, particularly in inaccessible or hazardous environments. A notable application is within the nuclear energy industry, where the long-term integrity of cable insulation and shielding is paramount to ensuring operational safety. In high-radiation zones, materials such as polymeric dielectrics degrade due to prolonged thermal stress and ionizing radiation exposure, leading to changes in their dielectric properties. Embedding IDC sensors within these environments enables remote, in-situ tracking of permittivity shifts, which serve as proxies for insulation wear, contamination, or material aging. This non-intrusive monitoring approach allows for predictive maintenance strategies, minimizing system downtime and enhancing overall reliability and safety.

In industrial process control, permittivity sensing via IDC structures offers valuable insights into the composition and quality of materials. For instance, in the oil and gas sector, the relative permittivity of multiphase fluids—such as oil–water emulsions—can be monitored to determine phase composition and separation efficiency. In agriculture and food processing, IDC sensors can detect moisture content in grains and powders, which is crucial for ensuring product quality, shelf life, and regulatory compliance. Similarly, in pharmaceutical manufacturing and polymer processing, IDC sensors enable real-time monitoring of the curing or drying states of compounds, ensuring consistency and reducing waste.

Across these diverse applications, IDC sensors are valued for their compact size, low cost, and compatibility with standard printed circuit board (PCB) fabrication techniques. Their ability to deliver accurate, real-time permittivity measurements in challenging environments positions them as a versatile solution for both applied research and commercial deployment in health diagnostics, industrial automation, and safety-critical monitoring systems.

10 Bonus Part: IDC with Spiral Inductor

The design of our Interdigitated Capacitor (IDC) sensor, optimized for a resonant frequency of 2.4, is inspired by the work of Porwal et al. [6], who developed a planar resonant RF sensor for simultaneous detection of complex permittivity and permeability using a combination of IDC and spiral inductors operating in the 2.2 to 2.8 band. Their sensor, fabricated on a 1.6 FR4 substrate, utilized a two-pole filter topology with IDC

and spiral inductors to differentiate permittivity and permeability based on odd and even mode resonant frequencies.

To adapt their design for our application, we modified the sensor to resonate at 2.4 using ANSYS HFSS simulations. Key changes include:

- **Substrate**: Retained FR4 with $\varepsilon_r = 4.4$, but reduced dimensions to $22 \times 15 \times 1.6$ for compactness while ensuring field containment.
- **Finger Dimensions**: Adopted $L = 10$, $W = 1$, and depth $= 0.1$, consistent with Porwal et al., to maintain capacitance and control conductive losses.
- **Number of Fingers**: Reduced to $N = 8$ from their $N = 6$ to increase capacitance, thereby tuning the resonant frequency to 2.4 and enhancing sensitivity.
- **Ports**: Configured wave ports for S-parameter extraction (S_{11} and S_{21}), aligning with their methodology for analyzing reflection and transmission characteristics.

These modifications ensure the sensor operates effectively at 2.4 while maintaining the nondestructive sensing capabilities demonstrated by Porwal et al. for RF applications.

Plots and Simulations link

11 Bonus Part: Design and Analysis of IDC Sensor for 5 GHz Resonance

This section presents the design and theoretical analysis of an Interdigitated Capacitor (IDC) sensor optimized to resonate at 5, suitable for RF sensing applications in the ISM band. The design involves calculating capacitance, inductance, sensitivity, and quality factor, with parameters adjusted to meet the target resonance.

11.1 Design Parameters

The IDC sensor is designed with the following initial parameters:

Table 3: Initial Design Parameters for 5 GHz IDC Sensor

Symbol	Description	Value
L	Length of finger	4.5
W	Width of finger	0.3
S	Spacing between fingers	1.6
N	Number of fingers	9
h	Height of substrate	0.8
ε_r	Dielectric constant	4.4 (FR4)

The substrate dimensions are 5×5. The initial design required adjustment to achieve the exact 5 resonance.

11.2 Theoretical Calculations

11.2.1 Capacitance Calculation

The total capacitance is calculated using:

$$C_{\text{total}} = 4(N-1)\varepsilon_0 L \left[\frac{K(k)}{K(k')} + \varepsilon_r \frac{K(k_1)}{K(k_1')}\right]$$

Where:

- $k = \frac{S}{S+2W} = \frac{1.6}{1.6+2\cdot 0.3} \approx 0.7273$
- $k_1 = \frac{\sinh\left(\frac{\pi W}{4h}\right)}{\sinh\left(\frac{\pi(S+2W)}{4h}\right)} \approx 0.0694$
- $\varepsilon_0 = 8.854 \times 10^{-12}\,\text{F/m}$, $\varepsilon_r = 4.4$
- $K(k)/K(k') \approx 1.062$, $K(k_1)/K(k_1') \approx 0.4146$

For $N = 9$:

$$C_{\text{total}} = 4 \cdot 8 \cdot 8.854 \times 10^{-12} \cdot 4.5 \times 10^{-3} \cdot [1.062 + 4.4 \cdot 0.4146]$$
$$\approx 3.676 \times 10^{-12}\,\text{F} = 3.676\,\text{pF}$$

11.2.2 Resonance Frequency and Inductance

The resonant frequency is:

$$f_{\text{res}} = \frac{1}{2\pi\sqrt{L_{\text{eff}} C_{\text{eff}}}}$$

For $C_{\text{eff}} = 3.676\,\text{pF}$ and $f_{\text{res}} = 5$:

$$L_{\text{eff}} \approx 0.2755\,\text{nH}$$

11.2.3 Parameter Optimization

To achieve 5, the number of fingers was increased to $N = 10$:

$$C_{\text{total}} = 4 \cdot 9 \cdot 8.854 \times 10^{-12} \cdot 4.5 \times 10^{-3} \cdot 2.886 \approx 4.593\,\text{pF}$$
$$L_{\text{eff}} \approx 0.2206\,\text{nH}$$
$$f_{\text{res}} \approx 5$$

Updated parameters:

11.3 Simulation Setup

The IDC sensor is prepared for simulation in ANSYS HFSS with:

- **Substrate**: FR4 ($\varepsilon_r = 4.4$), $5 \times 5 \times 0.8$.
- **Finger Dimensions**: $L = 4.5$, $W = 0.3$, depth $= 0.1$.
- **Number of Fingers**: $N = 10$.
- **Ports**: Two wave ports with 50 impedance.
- **Air Box**: Models free-space boundary conditions.

A parametric sweep on N and L can fine-tune the resonance.

Table 4: Updated Design Parameters for 5 GHz IDC Sensor

Symbol	Description	Value
L	Length of finger	4.5
W	Width of finger	0.3
S	Spacing between fingers	1.6
N	Number of fingers	10
h	Height of substrate	0.8
ε_r	Dielectric constant	4.4

11.4 Sensitivity Analysis

Sensitivity to dielectric changes is evaluated with a 0.2 analyte layer:

$$f_r \propto \frac{1}{\sqrt{\varepsilon_{\text{eff}}}}$$

Estimated resonant frequencies:

Table 5: Effect of Analyte Permittivity on Resonant Frequency

Analyte	Relative Permittivity (ε_r)	Resonant Frequency ()
Air	1	5.6
Polyester	3.2	5.2
Silicon	11.7	4.6
Water	80	3.8

Sensitivity:

$$S = \frac{\Delta f}{\Delta \varepsilon_r} = \frac{|5.6 - 5.2|}{|1 - 3.2|} = \frac{0.4}{2.2} \approx 0.18\,\text{GHz}/\varepsilon_r$$

11.5 Quality Factor

The quality factor is:

$$Q = \frac{1}{\omega C R_{\text{loss}}}$$

For $\omega = 2\pi \cdot 5 \times 10^9$, $C = 4.593 \times 10^{-12}\,\text{F}$, $R_{\text{loss}} = 0.1\,\Omega$:

$$Q \approx 69.3$$

11.6 Results

The IDC sensor achieves:

- **Capacitance**: 4.593 pF
- **Inductance**: 0.2206 nH
- **Resonant Frequency**: 5
- **Sensitivity**: $\approx 0.18\,\text{GHz}/\varepsilon_r$

Figure 21: 5GHZ plot

- **Quality Factor**: ≈ 69.3

The design is expected to meet S-parameter targets ($S_{11} < -10\,\text{dB}$, $S_{21} > -3\,\text{dB}$), making it suitable for RF sensing applications.

12 Acknowledgement

We would like to express our sincere gratitude to Professor Andleeb Zahra for her invaluable guidance and support throughout the duration of this course. We deeply appreciate her efforts in introducing this new and technically challenging subject at IIIT Hyderabad, and for expanding our understanding of it.

We are especially thankful to her for assigning this project, which provided us with a hands-on opportunity to explore sensor design using HFSS. This experience offered us foundational insights into the process of tape-out design and its subsequent fabrication.

We would also like to extend our thanks to the Teaching Assistant of the course for their consistent support and assistance in resolving the challenges we encountered while learning HFSS.

References

1. Introduction to ElectroDynamics Fourth Edition by David J. Griffiths
2. Elements of Electromagnetics by Matthew N. O. Sadiku
3. University of South Carolina Scholar Commons: Distributed Interdigital Capacitor (IDC) Sensing for Cable Insulation Aging and Degradation Detection by Md Nazmul Al Imran
4. P. V. V. Kishore and B. V. Sanker Ram, "Design of Microstrip IDC for Compact UWB BPF," *IJRET*, vol. 5, May 2016.
5. ANSYS, "HFSS Design Guide," 2015.
6. Design of RF Sensor for Simultaneous Detection of Complex Permeability and Permittivity of Unknown Sample : Pratik Porwal1, , Azeemuddin Syed, Prabhakar Bhimalapuram, and Tapan Kumar Sau

7. Solvent-Based Optimization of CSRR and IDC RF Bio-Sensors: Kunal Wadhwani, Associate Member, IEEE, Sheena Hussaini, Annesha Mazumder, Student Member, IEEE, and Azeemuddin Syed, Senior Member, IEEE

8. A label-free sensing of creatinine using radio frequency-driven labon-chip (LoC) system: Andleeb Zahra, Zia Abbas, Pawan Kumar, Swarnim Sinha, Alimpan Modak, Imran Siddiqui, Azeemuddin Syed, Prabhakar Bhimalapuram, and Tapan Kumar Sau

9. RF sensor-based tracking of nanoparticle's morphological and relative arrangement variations : Annesha MazumderTapan K. Sau, Syed Azeemuddin, Prabhakar Bhimalapuran

10. A Dual-Band Integrated Network Analyzer for Water Solvent-Specific RF Biosensors; Mayank Awasthi, Syed Azeemuddin, Senior Member, IEEE, Annesha Mazumder, and Mohammad Hashmi, Senior Member, IEEE